Journal of Geodesy (2000) 74: 503–511

Journal of Geodesy

A synthetic Earth for use in geodesy

R. Haagmans

Department of Mapping Sciences, The Agricultural University of Norway, PO Box 5034, N-1432 Ås, Norway
e-mail: roger.haagmans@ikf.nlh.no; Tel.: +47 64948846; Fax: +47 64948856

Received: 6 August 1999 / Accepted: 26 April 2000

Abstract. A synthetic Earth and its gravity field that can be represented at different resolutions for testing and comparing existing and new methods used for global gravity-field determination are created. Both the boundary and boundary values of the gravity potential can be generated. The approach chosen also allows observables to be generated at aircraft flight height or at satellite altitude. The generation of the synthetic Earth shape (SES) and gravity-field quantities is based upon spherical harmonic expansions of the isostatically compensated equivalent rock topography and the EGM96 global geopotential model. Spherical harmonic models are developed for both the synthetic Earth topography (SET) and the synthetic Earth potential (SEP) up to degree and order 2160 corresponding to a $5' \times 5'$ resolution. Various sets of SET, SES and SEP with boundary geometry and boundary values at different resolutions can be generated using low-pass filters applied to the expansions. The representation is achieved in point sets based upon refined triangulation of a octahedral geometry projected onto the chosen reference ellipsoid. The filter cut-offs relate to the sampling pattern in order to avoid aliasing effects. Examples of the SET and its gravity field are shown for a resolution with a Nyquist sampling rate of 8.27 degrees.

Key words: Gravity field – Synthetic Earth – Boundary values

1 Introduction

Within the International Association of Geodesy (IAG) the idea of the construction of a synthetic Earth has been encouraged in order to obtain a better insight into different methods that are applied in practice, mainly for the analysis of the Earth's global gravity field. There even exists an IAG special study group especially focusing on the topic of a synthetic Earth, but most of its goals are beyond the scope of this study. In this context, previous studies have been conducted, such as the mass-point geopotential modelling experiment by Vermeer (1995). The inspiration for this study partly originates from ideas presented in Van Gelderen (1991), who created a two-dimensional synthetic Earth. The aim of the current study is to realize an artificial Earth and its gravity field at various resolutions with a corresponding band-limited signal content. The latter is mainly done in order to avoid the procedures required for aliasing treatment that are common to most approaches in gravity-field determination, but this is not the main focus and the major interest in the aforementioned comparison of methods. For future needs, the case of non-band-limited signals can be easily obtained by following the same procedure, but simply changing the filter characteristics. The synthetic Earth is designed for the testing of gravity-field modelling methods exterior to the Earth's physical surface, such as comparison of boundary element methods (BEM) with least-squares (LS) collocation or spherical harmonic analysis with spherical wavelet analysis in preparation for gravity gradiometry missions.

The Earth's topography, i.e. orthometric heights, and geoid heights are combined to yield the Earth geometry relative to a chosen reference ellipsoid. The combination of the ellipsoid and the Earth geometry is called the synthetic Earth shape (SES). The gravity-field observables, such as the gradient vector of the gravity potential, are generated from a synthetic Earth potential (SEP) that is expanded in spherical harmonics up to degree and order 2160. Such a spherical harmonic model is constituted of the EGM96 model (Lemoine et al. 1997) and an isostatically compensated equivalent rock topography model (Rummel et al. 1988). Both the spherical harmonic coefficients of the topography and

Formerly at: Delft Institute for Earth-Oriented Space Research (DEOS), Delft University of Technology,
Thijsseweg 11, NL-2629JA Delft, The Netherlands

the topographic–isostatic potential are derived using the GETECH global $5' \times 5'$ digital terrain model (GETECH 1995). The combination of these coefficient sets using adequate low-pass filters, tuned to the desired spatial sampling pattern, leads to the mentioned SES and chosen boundary values from the SEP. The use of the spherical harmonic expansion also allows the generation of observables at the flight height of aeroplanes and at satellite altitudes.

The creation of the synthetic Earth topography (SET) will be discussed in the second section of this paper. The third section is devoted to the construction of the spherical harmonic coefficients of the SEP, followed by a section on the generation of the shape of the SES boundary and specific boundary values such as the elements of the gradient vector of the gravity potential.

2 The synthetic Earth topography (SET)

The Earth topography is derived from the GETECH global $5' \times 5'$ digital terrain model (GETECH 1995). The topography is considered as orthometric heights on land and depths over the oceans. From a global equiangular grid of 2160 elements in latitude and 4320 elements in longitude, spherical harmonic coefficients are obtained up to degree (n) and order (m) 2160 following a modification of the procedure described in Colombo (1981). For this purpose, algorithms and scaling as discussed in Koop and Stelpstra (1989) and in Koop (1993) are tested and applied in order to avoid numerical stability problems in the recurrence relations of the Legendre functions. Before a spherical harmonic expansion can be computed, a so-called equivalent rock topography is generated (cf. Rummel et al. 1988). This can be achieved by replacing all water depths (D) by a smaller negative topography consisting of rock, $H^{\mathrm{er}} = -0.614D$. The factor 0.614 results from the conversion of a column of water of constant density into rock of constant density equal to 2670/kg m^3. Next, the global topography with constant density everywhere can be expanded into a spherical harmonic series. The spherical harmonic analysis yields coefficients ($H_{nm\alpha}$) from the point equivalent rock topography values H^{er}

$$H_{nm\alpha} = \frac{1}{4\pi} \iint_{\sigma} \frac{H^{\mathrm{er}}(q)}{R} Y_{nm\alpha}(q) \mathrm{d}\sigma_q \tag{1}$$

where

$$Y_{nm\alpha}(q) = \bar{P}_{nm}(\sin \varphi_q) \begin{cases} \cos m\lambda_q & \text{for } \alpha = 0 \\ \sin m\lambda_q & \text{for } \alpha = 1 \end{cases}$$

and the integration is performed over all points q on the unit sphere σ; φ and λ are the geocentric latitude and longitude, and $\bar{P}_{nm}$ are the fully normalized associated Legendre functions. The heights/depths become dimensionless after division by the mean Earth spherical radius (R). From these coefficients, the Earth topography at an arbitrary point p can be reconstructed from a spherical harmonic synthesis up to the maximum degree $N_{\max} = 2160$ using

$$H^{\mathrm{er}}(p) = R \sum_{n=0}^{N_{\max}} \sum_{m=0}^{n} \sum_{\alpha=0}^{1} H_{nm\alpha} Y_{nm\alpha}(p) \tag{2}$$

and the equivalent rock topography can be converted back to water depth by $D = -H^{\mathrm{er}}/0.614$ in the case of $H^{\mathrm{er}} < 0$.

The analysis strategy for solving the discretized version of Eq. (1), according to Colombo (1981), allows the use of point data or mean data. The point-data approach was used, which may cause imperfections in a range of degrees of the expansion. This is mainly due to the lack of a one-to-one relation between the number of grid points and the coefficients (it is approximately 2:1). The result is that a $5' \times 5'$ topography grid created from the spherical harmonic coefficients does not exactly match the original GETECH $5' \times 5'$ at the smallest scales. In areas with the most extreme topographic gradients, the maximum differences can be of the order of several tens of metres. However, this is of no importance for the creation of the *synthetic* Earth as the space domain result of the spherical harmonic synthesis is adopted as a 'true' world topography, and the original GETECH data set is no longer used.

3 The gravity potential of the synthetic Earth (SEP)

As well as the topography that is needed to define one part of the boundary, a 'realistic' potential field must also be created. The idea is to use an existing global geopotential model for the lower degrees, in combination with adapted geopotential coefficients obtained from a global topographic–isostatically-induced potential for the medium and smaller-scale details. This procedure will be explained in the three steps below. First, the use of the global geopotential model is discussed, followed by a description of the topographic–isostatic potential, and finally the adaptation procedure for combining both models is presented.

The EGM96 global geopotential model (Lemoine et al. 1997) is chosen. The coefficients, provided in a tide-free system, are converted to refer to the GRS80 ellipsoid (Moritz 1980) using the ratios between the GM values i.e. the geocentric gravitational constants and the semi-major axis a as described in, for example, De Bruijne et al. (1997). For the representation of the longer-wavelength contents of the SEP, the EGM96 coefficients ($C^{\mathrm{EGM}}_{nm\alpha}$) are low-pass filtered using a spherical equivalent of the Butterworth filter $F(\psi)$ (see e.g. Oppenheim et al. 1983) with the spectral amplitude filter coefficients B_n. This Butterworth filter is as follows:

$$F(\psi_{pq}) = \sum_{n=0}^{\infty} (2n+1) B_n(n_{\mathrm{b}}, k) P_n(\cos \psi_{pq}) \tag{3}$$

and

$$B_n(n_{\mathrm{b}}, k) = \sqrt{\frac{1}{1 + \left(\frac{n}{n_{\mathrm{b}}}\right)^{2k}}}$$

where k is the order of the filter, n_{b} is the band degree at which the power is halved (or the amplitude $\sqrt{2}/2$), ψ_{pq}

is the spherical distance between the points p and q, and $P_n(\cos\psi)$ are the non-normalized Legendre polynomials (Heiskanen and Moritz 1967). The low-pass filter characteristics are chosen as $n_b = 50$ and $k = 3$ from degree 2 up to 360 in order to suppress the weights for the amplitude towards zero for the degrees tending to 360. This is needed for a smooth transition between the EGM96 potential coefficients and the topographic–isostatic-induced potential that is treated with the complementary filter, thus with weights close to one just over degree 360. This is closely related to the choices in the weighing procedures of modified Stokes approaches (cf. Haagmans et al. 1998). This choice of the filter characteristics also implies that most of the energy in the coefficients of EGM96 up to degree 50 is kept, and beyond 50 is suppressed. Accordingly, the filtered coefficients are

$$C^{\mathrm{LP}}_{nm\alpha} = B_n(50,3)C^{\mathrm{EGM}}_{nm\alpha} \quad \text{for } n = 2,\ldots,360 \tag{4}$$

These coefficients describe the gravity potential caused by deeper and/or larger-scale mass inhomogeneities inside the Earth. An example of a Butterworth spectral filter with $n_b = 150$ and $k = 3$ is shown in the right-hand-side plot of Fig. 1. The power per degree (c_n) for the dimensionless spherical harmonic coefficients ($C_{nm\alpha}, S_{nm}$), such as those of the topography or potential in Eqs. (1) and (4), can be expressed by a degree variance spectrum as

$$c_n = \sum_{m=0}^{n}\sum_{\alpha=0}^{1} C^2_{nm\alpha} = \sum_{m=0}^{n}(C^2_{nm} + S^2_{nm}), \quad n \geq 0 \tag{5}$$

The complementary part of the potential coefficients and the extension up to degree and order 2160 is derived starting from a potential caused by the SET and its isostatic compensation. As a first step, potential coefficients based solely upon an isostatically compensated equivalent rock topography are generated following the procedure described in Rummel et al. (1988). It consists of the following steps.

1. Spherical harmonic coefficients $H_{nm\alpha}$, $H2_{nm\alpha}$ and $H3_{nm\alpha}$ are determined from the global $5' \times 5'$ GETECH grids with equivalent rock topography for H/R, $(H/R)^2$ and $(H/R)^3$, respectively. The latter terms replace H/R in Eq. (1) to obtain the second and third set of coefficients from degree 0 up to 2160. The use of the third-order approximation beyond degree 180 as applied in Rummel et al. (1988) may lead to too high an energy in the highest degrees of the expansion for the potential, however this will be reduced in the combination procedure described hereafter.
2. For the isostatic compensation, an Airy–Heiskanen model is chosen with a compensation depth (D_c) of 30 km. However, the compensation is not likely to be valid for topographic signals at spatial scales smaller than 200 km. The spectral compensation component is therefore low-pass filtered with a Butterworth filter $B_n(150, 3)$; see Eq. (3).
3. The topographic and isostatic components are combined to give dimensionless spherical harmonic coefficients $C^{\mathrm{TI}}_{nm\alpha}$.

The result of these three steps is, for $n = 2,\ldots,2160$

$$\begin{aligned} C^{\mathrm{TI}}_{nm\alpha} = \frac{3}{2n+1}\frac{\rho_c}{\rho_e}\Bigg\{ & \left[1 - B_n(150,3)\left(\frac{R-D_c}{R}\right)^n\right]H_{nm\alpha} \\ & + \frac{n+2}{2}\left[1 + B_n(150,3)\frac{\rho_c}{\Delta\rho}\left(\frac{R-D_c}{R}\right)^{n-3}\right]H2_{nm\alpha} \\ & + \frac{(n+2)(n+1)}{6} \\ & \times \left[1 - B_n(150,3)\frac{\rho_c^2}{\Delta\rho^2}\left(\frac{R-D_c}{R}\right)^{n-6}\right]H3_{nm\alpha}\Bigg\} \end{aligned} \tag{6}$$

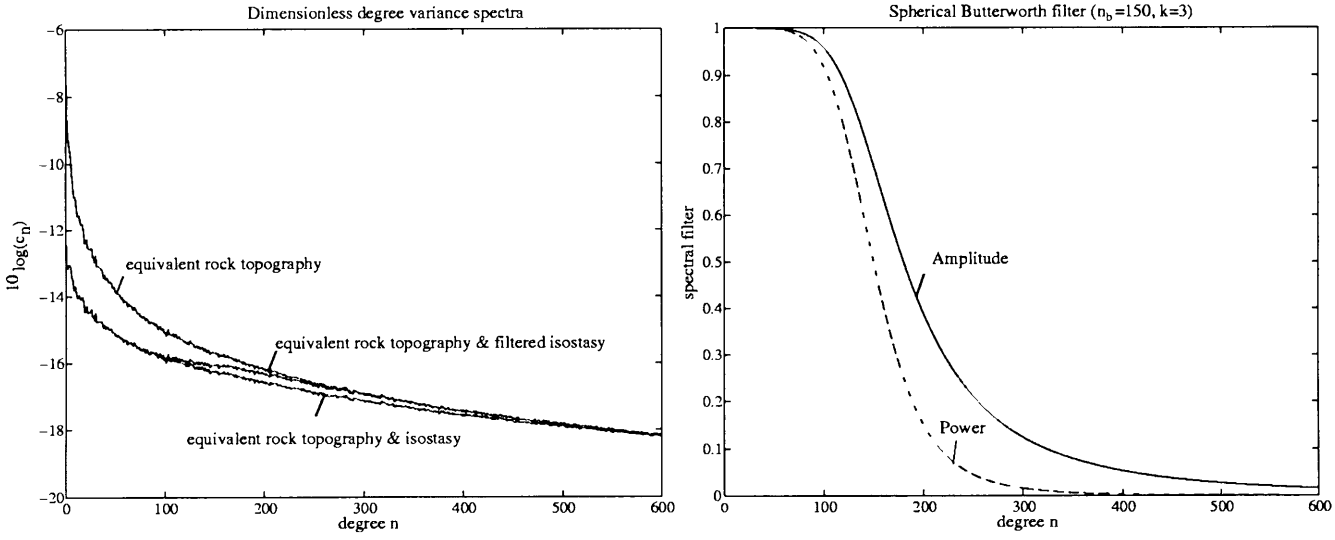

Fig. 1. Degree variances of topography and isostasy combinations (*left*); the isostasy low-pass filter (*right*)

where $\rho_e = 5514$ kg/m^3 is the mean density of the Earth (Rummel et al. 1988) and $\rho_c = 2670$ kg/m^3 is the mean density of the crust; $\Delta\rho = \rho_m - \rho_c = 3270 - 2670 = 600$ kg/m^3 is the density contrast between the mantle and the crust at the root of the isostatic compensation. The degree variance spectra of equivalent rock topography, of equivalent rock topography and its isostatic compensation, and of the Butterworth-filtered version of the latter (including the filter) are shown in Fig. 1. More details and discussion on the choice and the background to this Earth model can be found in Rummel et al. (1988).

Now, two potential coefficient sets are available for an overlapping frequency range between degrees 2 and 360. Since the topographic-isostatic potential does not contain contributions from deep mass inhomogeneities, except those of topography, the degree variances do not match the degree variances of the model Earth from EGM96, which is based on observational data. Instead of modelling all other mass inhomogeneities, rather than those caused only by the topography, an empirical approach was chosen to force a match between the degree variance spectra. Between degrees 25 and 360, linear trends are LS fitted to the logarithmic degree variance spectra $\log(c_n)$ of EGM96, obtained by substituting $C_{nm\alpha}^{\mathrm{EGM}}$ in Eq. (5), and of the topographic–isostatic model, obtained by substituting $C_{nm\alpha}^{\mathrm{TI}}$ in Eq. (5). This gives

$$\log(c_n^{\mathrm{EGM}}) - \log(c_n^{\mathrm{TI}}) = \Delta a + \Delta b n + \varepsilon$$
$$\Delta a = a_{\mathrm{EGM}} - a_{\mathrm{TI}} \quad \text{and} \quad \Delta b = b_{\mathrm{EGM}} - b_{\mathrm{TI}} \tag{7}$$

The difference in trend is applied to all topographic–isostatic coefficients in order to obtain an improved match between the degree variances in the overlapping range and a smooth extension to higher degrees, so that the corrected coefficients $C_{nm\alpha}^{\mathrm{TIC}}$ become for degree 2 to 2160

$$C_{nm\alpha}^{\mathrm{TIC}} = C_{nm\alpha}^{\mathrm{TI}} 10^{1/2(\Delta a + \Delta b n)} \tag{8}$$

Note that the factor of 1/2 occurs in Eq. (8) because Eq. (7) relates to power and Eq. (8) relates to magnitude.

At this stage, it is possible to combine the EGM96 low-pass filtered coefficients [Eq. (4)] with the coefficients of the corrected topographic–isostatic potential [Eq. (8)]. In order to obtain a smooth transition between the two sets, a high-pass Butterworth filter Bu_n was used for the corrected topographic–isostatic potential coefficients. That is, the complement in power of the low-pass filter is applied to EGM96, which gives

$$C_{nm\alpha}^{\mathrm{HP}} = Bu_n(50,3) C_{nm\alpha}^{\mathrm{TIC}} \quad \text{for } n = 2, \ldots, 2160$$
$$Bu_n(n_b, k) = \sqrt{1 - B_n^2(n_b, k)} \tag{9}$$

Combining the results of Eqs. (4) and (9) leads to the dimensionless potential coefficients ($C_{nm\alpha}$) defining the SEP. This approach leads to an Earth potential model that has a similar behaviour to EGM96 in terms of its spectral power, with a smooth extension up to degree and order 2160. Therefore

$$C_{nm\alpha} = C_{nm\alpha}^{\mathrm{LP}} + C_{nm\alpha}^{\mathrm{HP}} \quad \text{for } n = 2, \ldots, 360$$
$$C_{nm\alpha} = C_{nm\alpha}^{\mathrm{HP}} \quad \text{for } n = 361, \ldots, 2160 \tag{10}$$

The matching approach and its result are shown in Fig. 2.

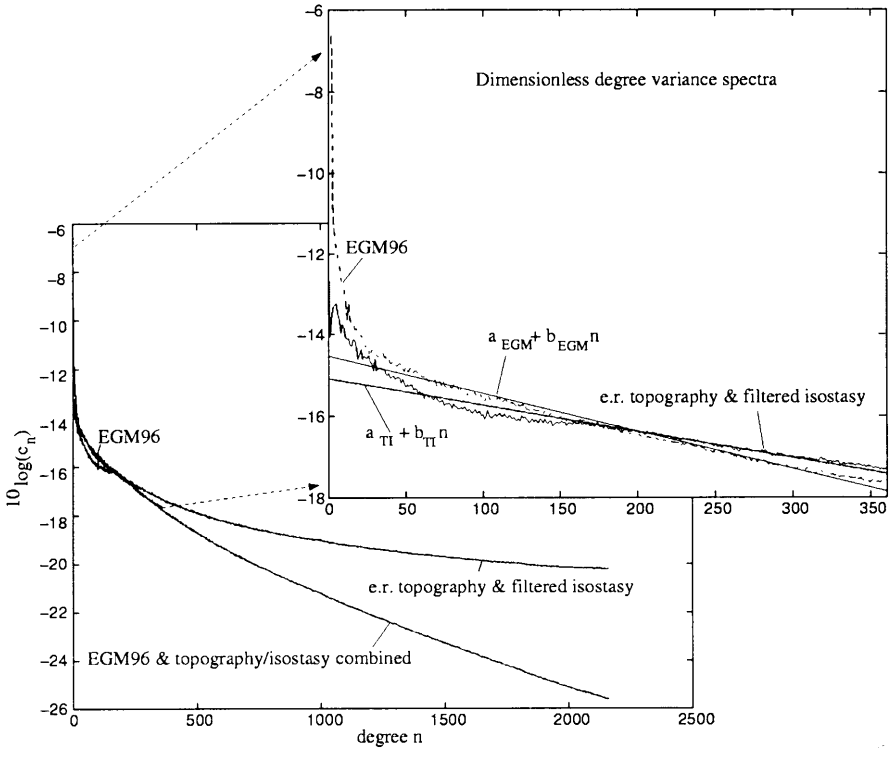

Fig. 2. Procedure for fitting equivalent rock (e.r.) topographic–isostatic degree variances to those of EGM96 (*right*), and the result of the final combined potential coefficient model (*left*)

A consequence of changing the topographic–isostatic potential coefficients by the empirically determined correction function is that the degree variances in the higher degrees become smoother, and loose the direct relation to the topographic–isostatic model as presented in Eq. (6); see Fig. 2. Obviously, the direct geophysical interpretation of the potential from the combined model is rather difficult and depends upon the filter parameters, and the meaning of the correction function. This means that the synthesized results from the model will, in a way, be 'realistic', and that it is not easy to invert the procedure applied. Thus, the effects of the assumptions that play a role in the topographic–isostatic model potential, for instance related to downward-continuation issues, are also difficult to trace back to the final model. The combined potential coefficients are the basis of the SEP that can be evaluated at arbitrary points by means of a spherical harmonic expansion.

4 The synthetic Earth shape (SES)

For every arbitrary point p on the GRS80 ellipsoid with geographical latitude Φ and longitude λ, Eq. (2) can be evaluated using the corresponding geocentric coordinates to yield an orthometric height $H(p)$ equal to $H^{\mathrm{er}}(p)$ on land. At sea, the boundary follows the shape of the mean sea surface. In this study, it is assumed that the mean sea surface coincides with the geoid, so that the height $H(p)$, denoting the permanent sea surface topography, is simply set to zero. An evaluation point p is defined to be situated at sea, when bathymetry $(-D)$ is present at that location. At the same point p, a spherical harmonic expansion can be evaluated to give geoid heights $N(p)$ using the potential coefficients in Eq. (10), with radius r_p from the origin of the ellipsoid to point p at the ellipsoid; this gives

$$N(p) = \frac{GM}{\gamma a}\sum_{n=2}^{N_{\max}}\left(\frac{a}{r_p}\right)^{n+1}\sum_{m=0}^{n}\sum_{\alpha=0}^{1}\Delta C_{nm\alpha}Y_{nm\alpha}(p) \tag{11}$$

and

$$\begin{cases}\Delta C_{nm\alpha} = C_{nm\alpha} - C_{nm\alpha}^{\mathrm{GRS80}} & \text{for } n = 2,4,6,8;\ m = 0;\ \alpha = 0\\ \Delta C_{nm\alpha} = C_{nm\alpha} & \text{otherwise}\end{cases}$$

where γ denotes the normal gravity at the ellipsoid (see e.g. Moritz 1980). The ellipsoidal height $h(p) = H(p) + N(p)$ for arbitrary points p at the ellipsoid can now be constructed. The ellipsoidal geometric heights, together with the GRS80 ellipsoid, define the shape of the SES boundary.

5 Construction of boundary values from the SEP

Once the shape of the SES boundary is generated, gravity-field quantities can be evaluated on or outside this boundary in order to obtain the desired potential field values and gravity observables, such as the disturbing potential $T(p)$ and the gravity acceleration magnitude (Heiskanen and Moritz 1967). In order to arrive at these values at the boundary at point p with geographic coordinates $\{\Phi, \lambda, h\}$ and corresponding geocentric coordinates $\{\varphi, \lambda, r\}$, the disturbing potential is first generated.

$$T(p) = \frac{GM}{a}\sum_{n=2}^{N_{\max}}\left(\frac{a}{r_p}\right)^{n+1}\sum_{m=0}^{n}\sum_{\alpha=0}^{1}\Delta C_{nm\alpha}Y_{nm\alpha}(p) \tag{12}$$
$$T(p) = W(p) - U(p)$$

In Eq. (12), $W(p)$ is the desired gravity potential at point p, and $U(p)$ is the normal gravity potential of the ellipsoidal field that can be obtained from (Heiskanen and Moritz 1967)

$$U(p) = V(p) + \Omega(p) \tag{13}$$

where

$$V(p) = \frac{GM}{r_p}\left[1 - \sum_{n=1}^{4}J_{2n}\left(\frac{a}{r_p}\right)^{2n}P_{2n}(\sin\varphi_p)\right]$$

and

$$\Omega(p) = \tfrac{1}{2}\omega^2(r_p\cos\varphi_p)^2$$

where J_{2n} are the non-normalized even zonal spherical harmonic coefficients of GRS80; ω is the Earth's constant rotation rate for GRS80 (cf. Moritz 1980); and $P_{2n}(\sin\varphi)$ are the non-normalized associated Legendre functions. Thus, Ω is the centrifugal potential. By combining the results of Eqs. (12) and (13), we are able to generate 'true' synthetic gravity potential values at arbitrary points on or outside the SES boundary.

Next, the focus is directed to the components of the gradient of T in the north direction along the x'-axis, in the east direction along the y'-axis, and in the zenith direction along the z'-axis. The latter coincides with the direction of r_p. The x'- and y'-axes are both tangential to the sphere of radius r_p. The gravity gradient vector can be obtained from differentiation of the disturbing potential $T(p)$ [Eq. (12)] in the three above-mentioned directions. The local Cartesian coordinates directly relate to the spherical coordinates at point p. The result for the gradient of T expressed in both coordinate systems is given in Eq. (14). More details on the elaboration of, for instance, the derivatives of the associated Legendre functions, can be found in Heiskanen and Moritz (1967).

$$\nabla T(p) = \left(\frac{\partial T(p)}{\partial x'}, \frac{\partial T(p)}{\partial y'}, \frac{\partial T(p)}{\partial z'}\right)$$
$$\frac{\partial T(p)}{\partial x'} = \frac{\partial T(p)}{r_p\partial\varphi} = \frac{GM}{r_p^2}\sum_{n=2}^{N_{\max}}\left(\frac{a}{r_p}\right)^{n}\sum_{m=0}^{n}\sum_{\alpha=0}^{1}\Delta C_{nm\alpha}\frac{\partial Y_{nm\alpha}(p)}{\partial\varphi}$$
$$\frac{\partial T(p)}{\partial y'} = \frac{\partial T(p)}{r_p\cos\varphi_p\partial\lambda} \tag{14}$$

$$= \frac{GM}{r_p^2 \cos\varphi_p} \sum_{n=2}^{N_{\max}} \left(\frac{a}{r_p}\right)^n \sum_{m=0}^{n} \sum_{\alpha=0}^{1} \Delta C_{nm\alpha} \frac{\partial Y_{nm\alpha}(p)}{\partial \lambda}$$

$$\frac{\partial T(p)}{\partial z'} = \frac{\partial T(p)}{\partial r} = -\frac{GM}{r_p^2} \sum_{n=2}^{N_{\max}} (n+1) \left(\frac{a}{r_p}\right)^n \sum_{m=0}^{n} \sum_{\alpha=0}^{1} \Delta C_{nm\alpha} Y_{nm\alpha}(p)$$

The last step is to transform the gradient of Eq. (14) to the gradient in the local Cartesian system with the x- and y-axis now in the tangent plane to the ellipsoidal normal at point p pointing north and east, respectively, and the z-axis in the direction of the outer normal of the ellipsoid at point p. The y-axis coincides with the y'-axis and only a rotation needs to be carried out over the positive angle $\Delta\Phi = \Phi_p - \varphi_p$ in the northern hemisphere and over the negative angle in the southern hemisphere. Thus

$$\nabla T(p) = \begin{pmatrix} \frac{\partial T(p)}{\partial x} \\ \frac{\partial T(p)}{\partial y} \\ \frac{\partial T(p)}{\partial z} \end{pmatrix} = \begin{pmatrix} \cos\Delta\Phi & 0 & -\sin\Delta\Phi \\ 0 & 1 & 0 \\ \sin\Delta\Phi & 0 & \cos\Delta\Phi \end{pmatrix} \begin{pmatrix} \frac{\partial T(p)}{\partial x'} \\ \frac{\partial T(p)}{\partial y'} \\ \frac{\partial T(p)}{\partial z'} \end{pmatrix} \tag{15}$$

The gravity vector $\bar{\mathbf{g}}(p)$ can now be obtained at point p by adding the vector of the ellipsoidal normal field $\bar{\gamma}(p)$ to the gradient vector of T. The normal gravity vector at point p, $\bar{\gamma}(p) = (0,\ 0,\ \gamma_h)$, with geodetic coordinates $\{\Phi, \lambda, h\}$, can be obtained from (Heiskanen and Moritz 1967)

$$\gamma_{h_p} = \gamma_{h_p=0} \left(1 - \frac{2}{a}(1 + f + m - 2f\sin^2\Phi_p)h_p + \frac{3}{a^2}h_p^2\right) \tag{16}$$

where $\gamma_{h=0}$ is normal gravity at the ellipsoid that can be obtained for the GRS80 geodetic latitude of p from Somigliana's formula (Heiskanen and Moritz 1967), f is the geometrical flattening of the GRS80 ellipsoid, and m is the centrifugal force at the equator divided by the normal gravity at the equator (Heiskanen and Moritz 1967). For distant points at satellite height, γ can also be obtained from an extension of the expansion in Eq. (16), without the centrifugal effect, or from taking the full derivative [as in Eq. (14)] of the potential V in Eq. (13) rotated to the ellipsoidal normal direction [as in Eq. (15)]. Combining the results of Eqs. (15) and (16), or Eq. (15) and modified versions of Eqs. (16) or (13), gives the gradient vector at point p. On the boundary this is

$$\bar{\mathbf{g}}(p) = \nabla W = \nabla U + \nabla T = \bar{\gamma} + \nabla T = \left(\frac{\partial T(p)}{\partial x}, \frac{\partial T(p)}{\partial y}, \frac{\partial T(p)}{\partial z} + \gamma_{h_p}\right) \tag{17}$$

Equations (15), (16) and (17) produce the 'true' synthetic gradient of the synthetic Earth at arbitrary locations on and, slightly modified, outside the SES boundary.

6 The generation of SES and SEP at different spatial resolutions

The SES boundary and the boundary values of SEP are generated at rather homogeneously sampled patterns. For the sampling pattern, an octahedron is used as a starting point (cf. Lage 1996). Each of the eight constituent triangles can be subdivided into four equal-sized triangles as described in Klees (1997), and so on to obtain an increased spatial resolution. Subsequently, the corner points of these triangles are projected onto a sphere with radius a. In Fig. 3 this procedure is illustrated for a resolution level 4 geometry. The number of triangles (N_{tr}) for each level l ($l = 0, 1, 2, \ldots$) is $N_{\text{tr}} = 2^{(3+2l)}$. The number of corner points N_{cp} in this case also the evaluation points, is related to the number of triangles by $N_{\text{cp}} = 2 + N_{\text{tr}}/2$ (see Fig. 3).

Next, the spherical coordinates of the corner points are considered to be geocentric, from which the point configuration on the GRS80 ellipsoid, shown in Fig. 4, automatically follows.

The results for different resolution levels in terms of (1) the number of evaluation points, (2) the maximum distance between neighbouring points, (3) the corresponding Nyquist degree and (4) the chosen Butterworth low-pass filter parameters are shown in Table 1. The filter parameters relate to the largest triangle side, denoted 'Largest distance' in Table 1, or the corresponding Nyquist degree, that is present in each resolution. The band degree n_{b} is half of the Nyquist degree and, together with the chosen order of the filter, it will reduce the signal that may be very aliased.

The lower and higher levels are not mentioned here, since the first focus will be at levels 4 to 9 from a practical and computational point of view. However, the idea can be extended to higher levels if desired in the future. For each level, a set of low-pass-filtered SET

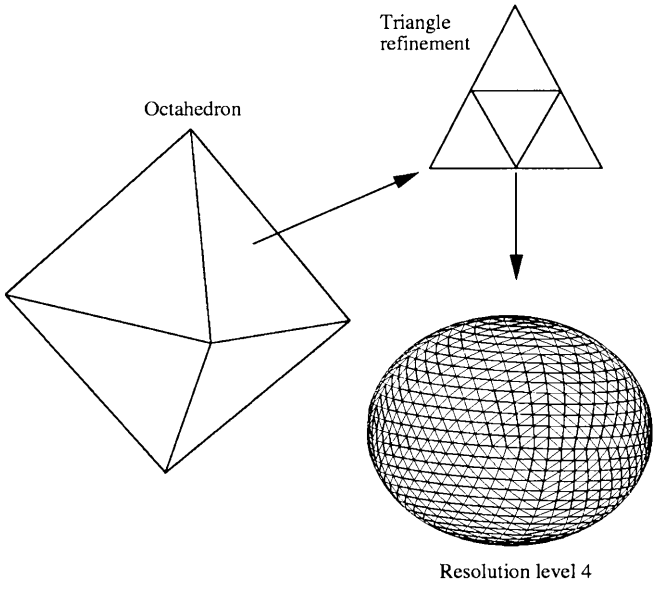

Fig. 3. Level 4 geometry from an octahedron and its refinement; 2048 triangles and 1026 points

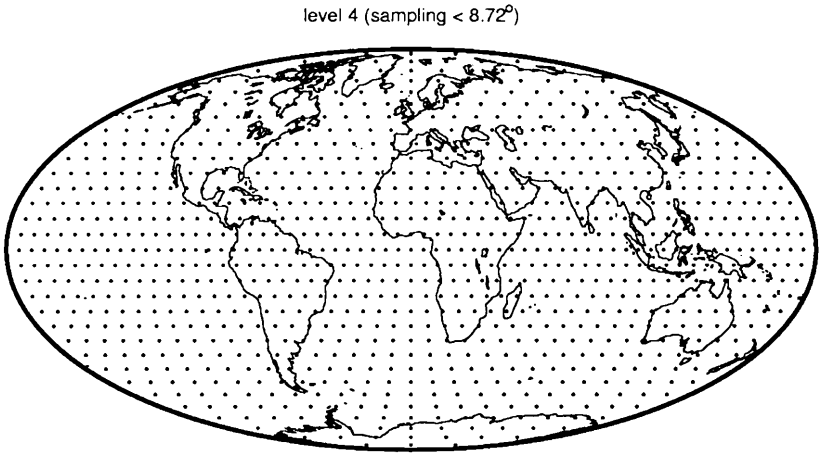

Fig. 4. Point distribution for level 4 resulting from the octahedron refinement

Table 1. Information on different resolution levels: the number of evaluation points, the largest occuring triangle side and the corresponding Nyquist degree, and the filter parameters

Resolution level	No. of points	Largest distance (deg)	Nyquist degree (≈)	Butterworth filter parameters
4	1026	8.72	20.5	$n_b = 10.25, k = 7$
5	4098	4.36	41	$n_b = 20.50, k = 7$
6	16 386	2.18	82	$n_b = 41.00, k = 7$
7	65 538	1.09	164	$n_b = 82.00, k = 7$
8	262 146	0.55	328	$n_b = 164.0, k = 7$
9	1 048 578	0.27	656	$n_b = 328.0, k = 7$

coefficients and SEP coefficients can be generated using the filter characteristics specified in Table 1. This means that $B_n(n_b, k)H_{nm\alpha}$ and $B_n(n_b, k)C_{nm\alpha}$ are used instead of $H_{nm\alpha}$ and $C_{nm\alpha}$ in Eqs. (2), (11), (12) and (14). These filters are chosen such that the effect of aliasing on the signal at higher degree than the Nyquist degree is small: for instance, for the topography at levels 7, 8 and 9, a signal-to-noise ratio of 10^{-4} was found, which means that the maximum errors in the topography are below 1 m. This seems acceptable since the original GETECH topography is provided in metres. As an example the topography–bathymetry, the disturbing potential and the gravity disturbance were generated at resolution level 4 [i.e. with $B_n(10.25, 7)$]. The gravity disturbance $\delta g(p) = -\partial T(p)/\partial r$ is obtained from Eq. (14) including the level 4 filter. The topography–bathymetry (i.e. orthometric heights and ocean depths) are shown in Fig. 5, the disturbing potential in Fig. 6 and the gravity disturbance in Fig. 7, for a level 4 global grid.

It is also possible to generate similar results, and the actual boundary with boundary values, for all the other mentioned resolutions. These can be made available for testing purposes to any interested group or individual. Information concerning the software and test data sets can be obtained from the author (deos@geo.tudelft.nl or roger.haagmans@ikf.nlh.no).

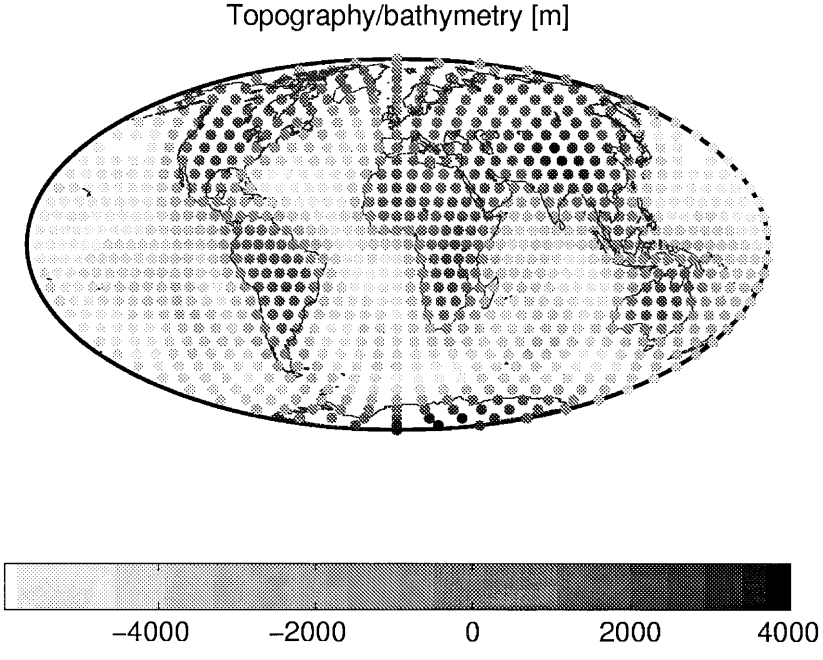

Fig. 5. Topography–bathymetry for level 4

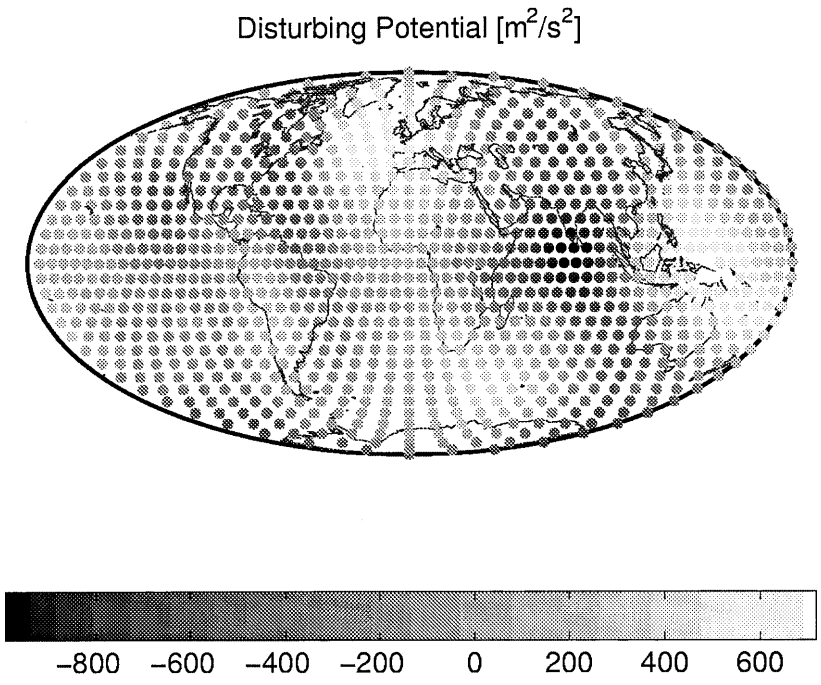

Fig. 6. Disturbing potential for level 4

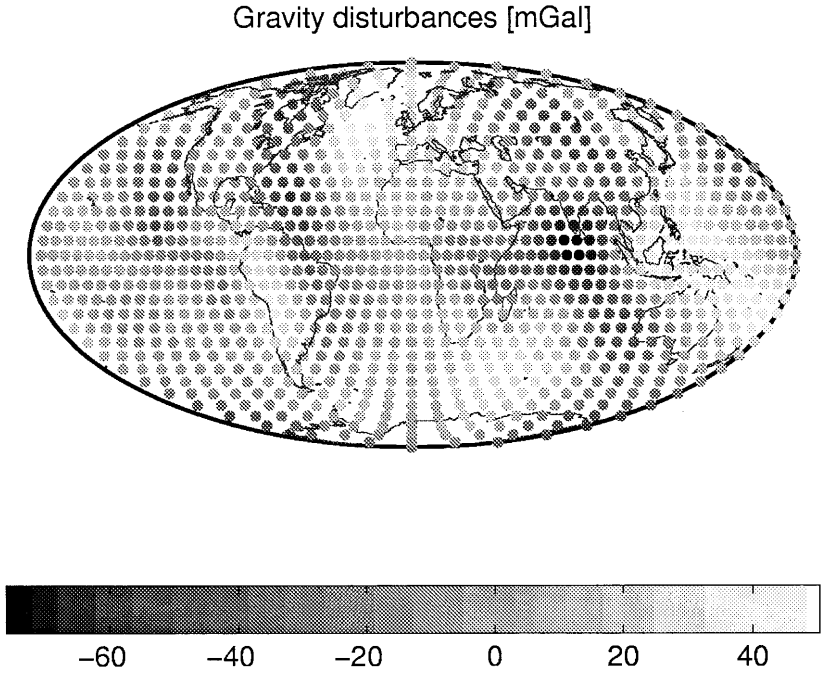

Fig. 7. Gravity disturbances for level 4

7 Summary and conclusions

In this study, a procedure has been presented and results are obtained for the creation of a synthetic Earth boundary and gravity-field boundary values. Part of the approach followed Van Gelderen (1991), who created a two-dimensional synthetic world. This required the adoption of a global topography with a fine resolution in order to be able to generate a 'realistic' potential field as an extension to the EGM96 model. In order to achieve this, a matching procedure in the spectral domain was developed and applied to the potential of the isostatically compensated equivalent rock topography in terms of spherical harmonic coefficients. Prescribing the spectral power of EGM96 in the range between degrees 25 and 360 to the final combined potential coefficients models, the results are expected to be reasonably close to reality, at least for the resolution levels 4 to 9 under consideration.

The development of the topography and potential in spherical harmonic coefficients allows, in combination with adequately chosen low-pass filters, rather straightforward representations of the SES boundary and the gravity field for the desired resolutions. For practical

representation, point sets are chosen based upon a triangulation scheme starting from an octahedron. The advantage of this scheme is the rather homogeneous sampling pattern on the Earth's surface. Butterworth filters are applied such that aliasing effects are minimal due to the link between the filter-band degree and the largest distance between neighbouring points of a chosen level. These filters can easily be changed, or even omitted, in order to allow aliasing to enter the problem. However, for the purpose of testing various techniques used in gravity-field practice, the alias-free synthetic realization of the Earth could be a good starting point.

Acknowledgements. The author would like to thank GETECH for providing the global $5' \times 5'$ digital terrain model, and NASA/NIMA for providing the EGM96 global geopotential model.

References

Colombo O (1981) Numerical methods for harmonic analysis on the sphere. Rep 310, Department of Geodetic Science and Surveying, The Ohio State University, Columbus

De Bruijne AJT, Haagmans RHN, De Min EJ (1997) A preliminary North Sea geoid model GEONZ97. MD-report MDGAP-9735, Survey Department Rijkswaterstaat, Delft

GETECH (1995) Global DTMS. Geophysical Exploration Technology (GETECH), University of Leeds

Haagmans RHN, De Bruijne AJT, De Min EJ (1998) A procedure for combining gravimetric geoid models and independent geoid data, with an example in the North Sea region. DEOS Prog Lett 98.1, DUP, Delft, pp 89–99

Heiskanen WA, Moritz H (1967) Physical geodesy. WH Freeman, New York

Koop R (1993) Global gravity field modelling using satellite gravity gradiometry. Publ 38, Netherland Geodetic Commission, Delft

Koop R, Stelpstra D (1989) On the computation of the gravitational potential and its first and second order derivatives. Manuscr Geod 14: 373–382

Klees R (1997) Topics on boundary element methods. In: Sansó F, Rummel R (eds) Lecture notes in Earth sciences 65. Geodetic boundary value problems in view of the one centimeter Geoid. Springer, Berlin Heidelberg New York, pp 482–533

Lage C (1996) Object oriented design aspects for boundary element methods. In: Hackbusch W, Wittum G (eds) Notes on numerical fluid mechanics, vol 54. Boundary elements implementation and analysis of advanced algorithms. Vieweg, Braunschweig, pp 159–170

Lemoine FG, Kenyon SC, Factor JK, Trimmer R, Pavlis NK, Chinn DS, Cox CM, Klosko SM, Luthcke SB, Torrence MH, Wang YM, Williamson RG, Pavlis EC, Rapp RH, Olson TR (1997) The development of the joint NASA GSFC and the National Imagery and Mapping Agency (NIMA) geopotential model EGM96. NASA/TP-1998-206861. GSFC Greenbelt, MD

Moritz H (1980) Geodetic reference system 1980. Bull Géod 54: 395–405

Oppenheim AV, Willsky AS, Young IT (1983) Signals and systems. Prentice-Hall International, Hemel Hempstead

Rummel R, Rapp RH, Sünkel H, Tscherning CC (1988) Comparisons of global topographic–isostatic models to the Earth's observed gravity field. Rep 388, Department of Geodetic Science and Surveying, The Ohio State University, Columbus

Van Gelderen M (1991) The geodetic boundary value problem in two dimensions and its iterative solution. Publ 35, Netherlands Geodetic Commission, Delft

Vermeer M (1995) Mass point geopotential modelling using fast spectral techniques; historical overview, toolbox description, numerical experiment. Manuscr Geod 20: 362–378